Electronic Supplementary Material (ESI) for ChemComm.

Supplementary Information

Rational Design of an Acceptor-Chromophore-Relay-Catalyst Tetrad Assembly for Water Oxidation

Experimental Procedures

Chemicals

All chemicals used in the experiments were employed as received without any additional purification. Cobalt(II) nitrate hexahydrate ($Co(NO_3)_2{\cdot}6H_2O$, 99%) and safranin O ($C_{20}H_{19}ClN_4$, >94%) were supplied by Fischer Scientific. Potassium chloride (KCl, 99–100%) and sodium persulfate ($Na_2S_2O_8$, >98%) were purchased from Sigma-Aldrich. The potassium phosphate buffer solution (PBS) was prepared by combining 0.1 M potassium phosphate monobasic (KH_2PO_4, Sigma-Aldrich, 98–100%) and 0.1 M potassium phosphate dibasic (K_2HPO_4, Sigma-Aldrich, >99%). Deionized water with a resistivity of 18 $M\Omega{\cdot}cm^{-1}$ was used throughout all experiments. Safranin O and fullerenol substances are referred to as [SF] and [F_{OH}], respectively, in this manuscript. Furthermore, the iron source $Na_3[Fe(CN)_5NH_3]$ is denoted as [Fe–NH_3] and synthesized following our previously published procedure.[1]

Synthesis of [F_{OH}]: 80 mg fulleren-C_{60} was dissolved in 50 mL toluene and then in 2 mL sodium hydroxide solution (1 g/mL), 5–6 drops of 30% hydrogen peroxide solution in water (40%), and 0.5 mL tetrabutyl ammonium hydroxide (40 wt% solution in water; Aldrich) as phase transfer catalyst were added, and the reaction mixture was stirred vigorously for 5 days at room temperature. The completion of the reaction was observed by the change in color of the organic phase. The forming [F_{OH}] was dissolved in water, and the organic phase became colorless. The organic solvent was removed, and [F_{OH}], was precipitated by the addition of ethanol to the aqueous phase. The filtrate was washed several times with ethanol, and the [F_{OH}] was obtained as a brown solid. The attachment of hydroxyl groups to the fullerene was confirmed by the presence of a broad peak at 3350 cm^{-1} in FT-IR spectrum (Figure S4).

Activation of [F_{OH}]: 60 mg [F_{OH}] was suspended in anhydrous *N,N*-dimethylformamide and sonicated for 1 hour to form a homogeneous suspension. Then the suspension was cooled to 0 °C, and 400 mg of *p*-nitrophenyl chloroformate, 2 mL of anhydrous pyridine, and a catalytic amount of *N,N*-dimethylaminopyridine were added to the solution. The reaction mixture was

stirred under nitrogen for 48 hours, together with 1 hour of sonication for every 8 hours of reaction. The activated [F_{OH}] was precipitated by the addition of diethyl ether, and then the obtained brown solid was washed with diethyl ether, dichloromethane, and isopropanol, respectively. The formation of activated [F_{OH}] was confirmed by the presence of aromatic doublets at 6.93 and 8.12 ppm in ^{1}H NMR spectroscopy.

Synthesis of [SF–Fe]: A 20 mL aqueous solution containing the organic photosensitizer, [SF], with a concentration of 0.03 M was added to a 20 mL aqueous solution of $Na_3[Fe(CN)_5NH_3]$ at the same concentration in a 1:1 stoichiometric ratio. The resulting mixture was stirred overnight at room temperature to generate the [SF–Fe] complex. Subsequently, the suspension was chilled in a refrigerator at +4 °C overnight to facilitate settling. It was then subjected to centrifugation at 6,000 rpm for 20 min to precipitate the [SF–Fe] complex, which was subsequently decanted. The resulting powder was dried for 2 days in an oven set at 75 °C.

Synthesis of [F_{OH}–SF–Fe]: 10 mg of the activated [F_{OH}] was dissolved in 5 mL of the anhydrous DMF and sonicated for 30 min. Then 28 mg of [SF–Fe] complex and 9 µL of *N,N*-diisopropylethylamine were added to the solution and stirred under nitrogen for 30 hours, together with 1 h of sonication for every 8 h of reaction. By the addition of diethyl ether, the precipitating claret red solid was washed with diethyl ether and dichloromethane containing 1-2 drops of methanol, respectively. The attachment of [SF] to [F_{OH}] was investigated by ^{1}H NMR and FT-IR spectroscopy methods and elemental analysis. The degree of functionalization of [SF–Fe] complex to [F_{OH}] was investigated using elemental analysis data. The number of [SF] groups was calculated by nitrogen percentage of the product. The percentage of nitrogen in [F_{OH}–SF–Fe] was found to be 19.19 and degree of functionalization was calculated as **8** per [F_{OH}].

Synthesis of [SF–Fe–Co]: [SF–Fe] was synthesized using a similar synthetic approach as described in our previous report.[2]

Synthesis of [F_{OH}–SF–Fe–Co]: A solution of [F_{OH}–SF–Fe] (0.03 M in 20 mL acetonitrile) was mixed with a solution of $Co(NO_3)_2$ (0.06 M in 20 mL ethanol) in a 2:1 ratio. The resulting solution was left to stir overnight at room temperature. The mixture was subsequently washed multiple times with cold ethanol and distilled water, followed by drying in an oven at 75 °C for 2 days. This process yielded the desired acceptor-chromophore-relay-catalyst tetrad assembly, referred to as [F_{OH}–SF–Fe–Co]. The obtained bulk precipitates were subsequently crushed using a mortar to obtain a powdered form suitable for further characterization and photocatalytic experiments.

Material Characterization

X-ray photoelectron spectroscopy (XPS) measurements were carried out using a Thermo Scientific K-Alpha XPS spectrometer utilizing Al K_α monochromatic radiation, ($h\upsilon$ = 1486.6 eV, 200 eV pass energy, 1 eV step size) and an electron flood gun for surface charge neutralization. The calibration of the binding energy (B.E.) scale was performed by fixing the adventitious C1s signal at 284.8±0.1 eV.

High-Resolution Field Emission Gun Scanning Electron Microscopy (SEM, FEI – Quanta 200 FEG) and Energy Dispersive X-ray Analysis (EDX) were used to characterize the atomic ratios of the samples and was operated at 15 kV. To confirm the formation of prepared complexes, we utilized a Bruker α Platinum-attenuated total reflection (ATR) spectrometer to measure Fourier-transform infrared spectroscopy (FTIR) spectra within the range of 4000−400 cm^{-1}, employing a 4 cm^{-1} resolution. We acquired ^{1}H nuclear magnetic resonance (NMR) spectra using a Varian Unity INOVA spectrometer operating at 500 MHz, maintaining the temperature at 25 °C. These spectra were recorded in DMSO solutions, and we utilized the nondeuterated solvent traces as an internal reference. The particle size of the powders in acetonitrile were measured at 298 K using Malvern-Zetasizer Nano, ZS. The measurements were repeated at least four times and polydispersity index (PDI)≤1 was taken. For the optical characterizations, UV-Vis-NIR spectrophotometer (Cary 300, Agilent Technologies) is employed and photoluminescence (PL) measurements have been performed using Cary Eclipse. The PL spectra for the solutions with 400 nm and 450 nm excitation wavelength. (~10^{-3} M in acetonitrile solutions, 2 mm cuvette length).

Femtosecond Transient Absorption Spectroscopy

A Ti:sapphire laser amplifier optical parametric amplifier system and 1 kHz repetition rate (Spectra Physics; Spitfire Pro XP; TOPAS) and a commercial pump probe experimental setup (Spectra Physics; Helios) with a white light continuum probe was used for the experiments. The pulse duration was measured as 120 fs by cross-correlation inside the pump probe setup. Pump beam wavelength was chosen as 520 nm according to the steady-state absorption spectra of studied compounds. A 2-mm thick cuvette containing the sample was used. The experimental data were analyzed by using the Surface Xplorer software supported by Ultrafast Systems.

Photocatalytic Experiments

Photocatalytic studies were performed on powder suspensions of samples in the presence of $Na_2S_2O_8$ as an electron scavenger at pH 7 under 1 sun illumination (100 mW/cm^2). To consume the electrons in the LUMO level of the PS upon photoexcitation, persulfate anion, $S_2O_8^{2-}$, is used as an efficient electron scavenger (ES), which has been commonly used in previous PB-based solar driven water oxidation studies.

A mixture of catalyst (5 mg) and $Na_2S_2O_8$ (20 mM) was dispersed in a 10 mL of phosphate buffer solution 50 mM ? (PBS) at pH 7 in a Pyrex cell. The suspension was sealed with a septum and degassed with N_2 gas for 30 min. prior to each photocatalysis. The reaction cell was irradiated with a solar light simulator (Sciencetech, Model SLB-300B, 300 W Xe lamp, AM 1.5 global filter) calibrated to 1 sun (100 mW cm^{-2}) under constant stirring and no leakage from air in the reaction flask was determined by monitoring the N_2 content. The amount of evolved oxygen in the headspace of the flask was sampled through the septum using a syringe and injected into gas chromatography (Agilent 7820A GC) equipped with a 5 Å molecular sieve column (Ar as the carrier gas) and a thermal conductivity detector (TCD). At least three samplings were conducted each time and the leakage control was provided by recording the N_2 amount. The standard error is calculated using the ratio of the standard deviation of

activities for each sampling hour to the square root of the number of samples, as depicted in the following equation:

$$\text{standard error} = \frac{\text{standard deviation of oxygen evolution for each sampling hour}}{\sqrt{\text{number of samples}}}$$

Turnover Number and Turnover Frequency Calculations

The turnover number (TON) was determined by dividing the moles of oxygen evolved from photocatalysis by the moles of cobalt present in the catalyst, assuming that all cobalt sites are active. To calculate the turnover frequency (TOF), which incorporates a time component in its definition, the TON is subsequently divided by the photocatalysis time.

$$\text{TON} = \frac{\text{the moles of evolved } O_2}{\text{the moles of Cobalt on compound}}, \text{TOF} = \frac{\text{TON}}{\text{time}}$$

Table S1. Atomic percentage of the compounds obtained from EDX and their derived chemical formulae.

Compound	**EDX atomic %**					
	Co	**Fe**	**C**	**N**	**O**	**Chemical Formula**
[F_{OH}–SF–Fe–Co]	4.74	3.27	51.30	24.05	16.64	$C_{60}(OH)_{18}(SF\text{-}Fe(CN)_5)_8Co_{10}(NO_3)_4.xH_2O$
[SF–Fe–Co]	6.64	5.69	43.01	36.02	8.63	$Co_{1.17}(Fe(CN)_5\text{-}SF)(NO_3)_{0.25}$

Table S2. Global fit results extracted from TA studies.

[SF–Fe–Co] (ps)	**[F_{OH}–SF–Fe–Co] (ps)**
0.7±0.3	0.29±0.09
19±14	68±43
Infinite	Infinite

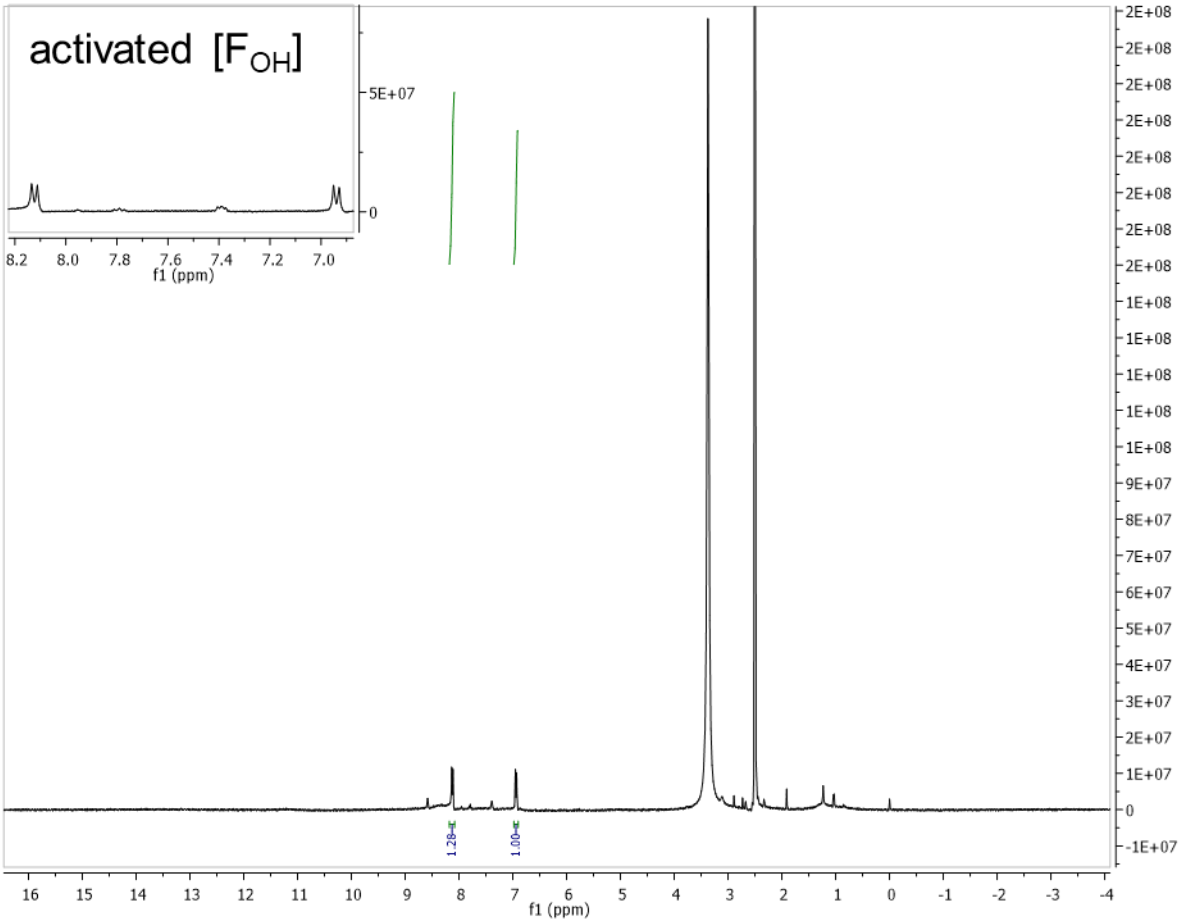

Figure S1. ^{1}H-NMR spectrum of crude activated [F_{OH}] (400 MHz, *DMSO-d_6*). δ 8.12 (d, 2H, *J* = 9.1 Hz), 6.93 (d, 2H, *J* = 9.1 Hz).

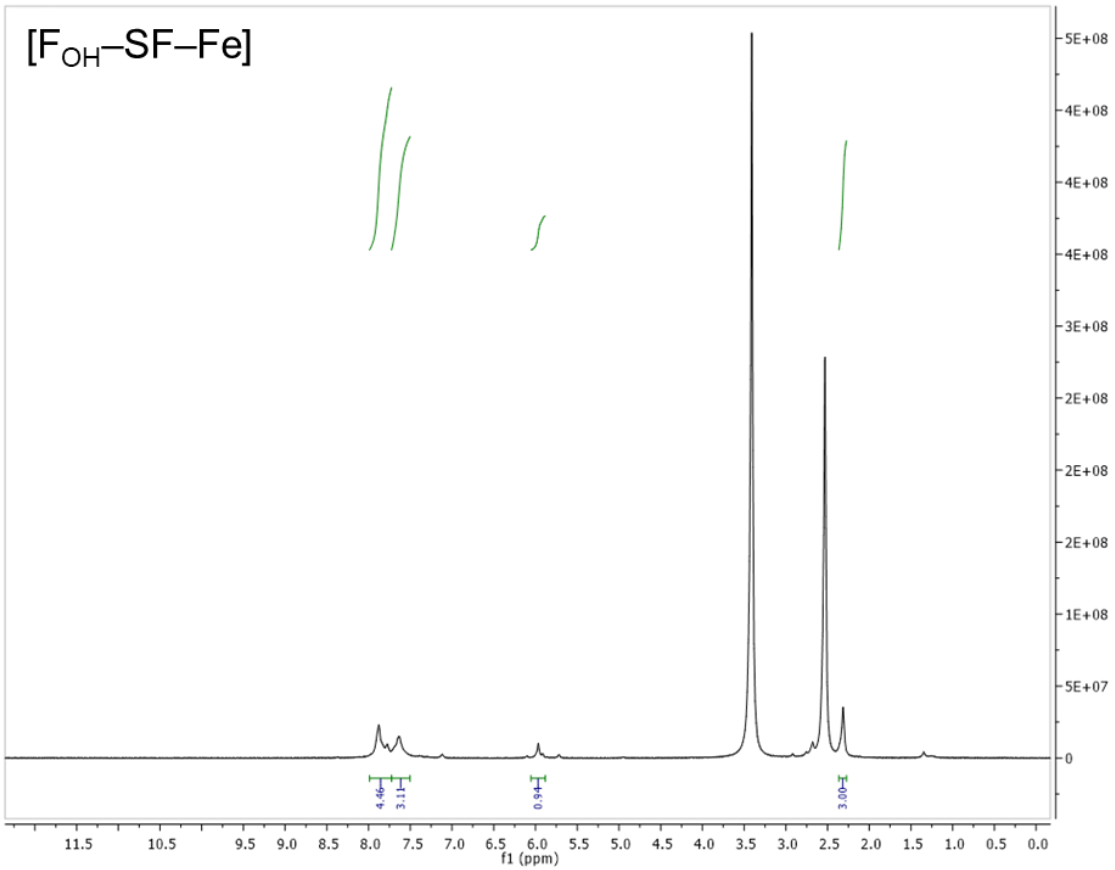

Figure S2. ^{1}H-NMR spectrum of [F_{OH}–SF–Fe] (400 MHz, *DMSO-d_6*). δ 7.90-7.75 (m, 5H), 7.65-7.45 (m, 3H), 5.97 (s, 1H) (overlapped with solvent residual peak), 2.31 (s, 3H).

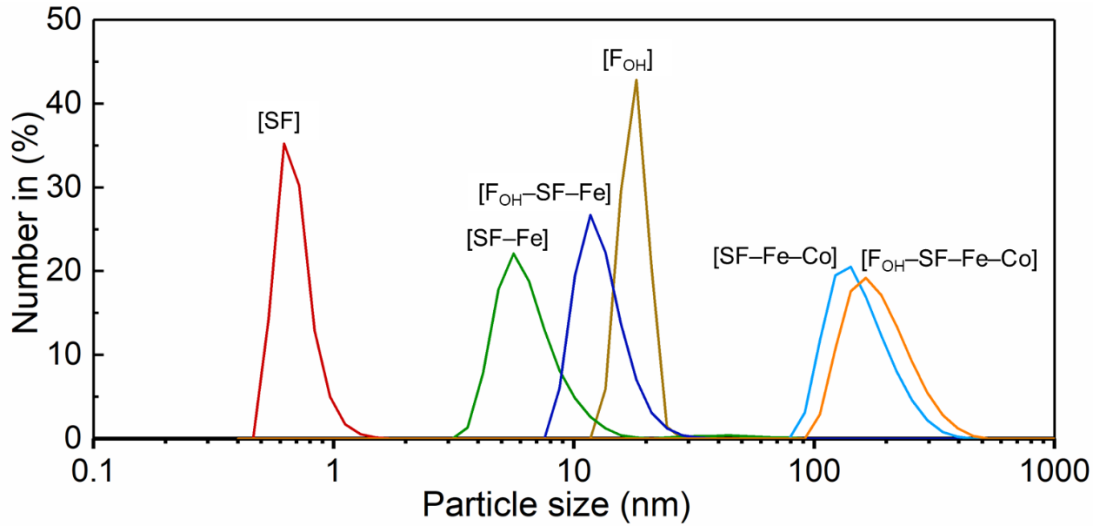

Figure S3. Particle size distribution based on dynamic light scattering (DLS) measurements

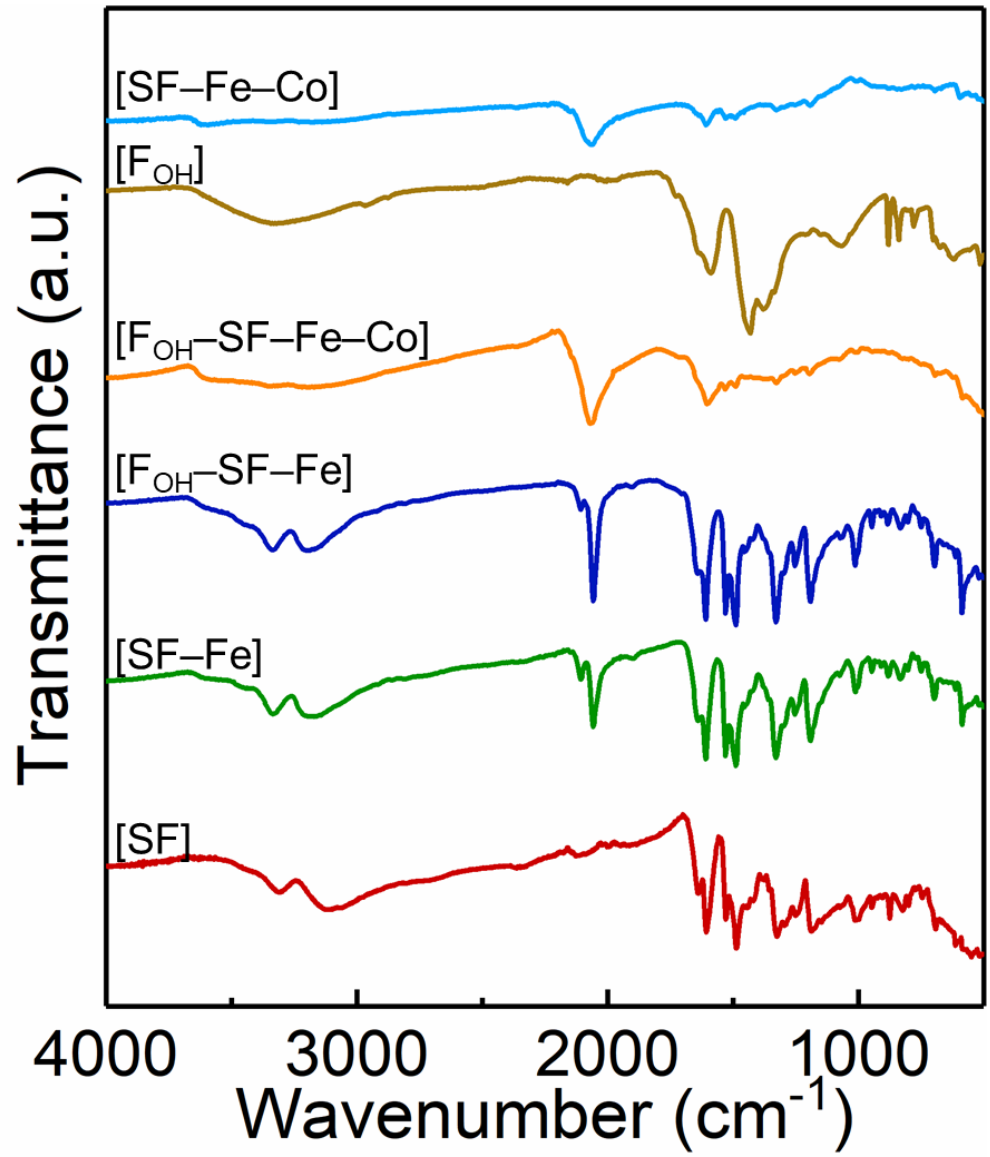

Figure S4. FTIR spectra of compounds.

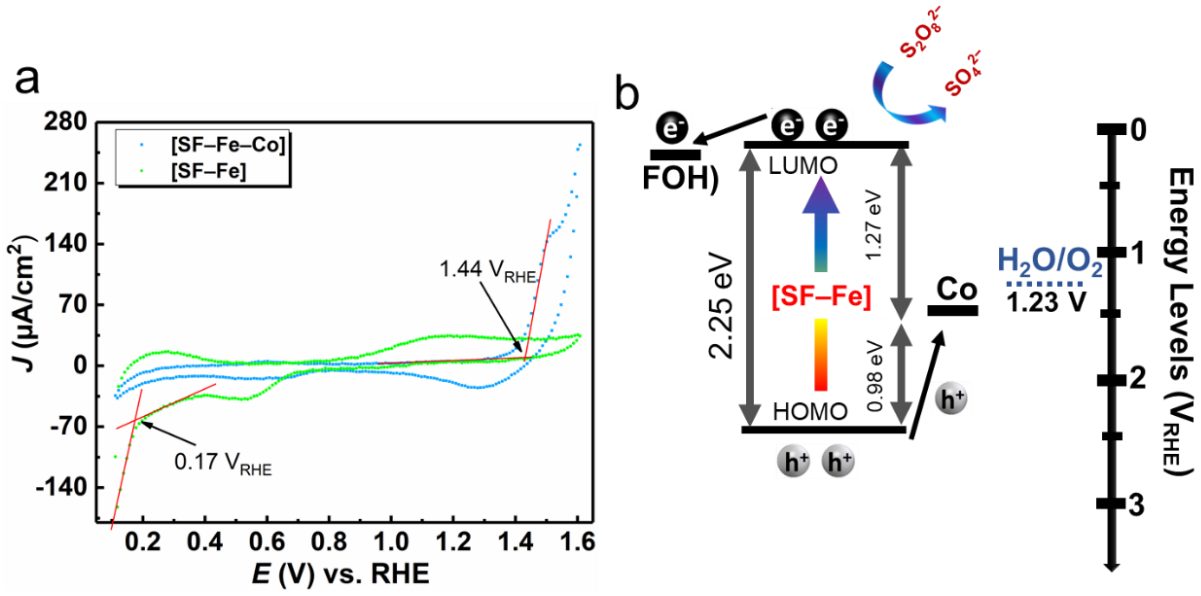

Figure S5. (a) The cyclic voltammograms of the homogeneous solutions of [SF–Fe] and [SF–Fe–Co] in N_2-saturated PBS solution (pH 7) at a scan rate of 500 mV/s. Fresh FTO coated glass was used as a working electrode, Ag/AgCl as a reference electrode, and Pt wire as a counter electrode (potential vs. RHE: $V_{RHE} = V_{Ag/AgCl}\,(V) + 0.059 \times pH + 0.1976$). Assigned reduction potential for [SF–Fe] is 0.17 V_{RHE}, and Co oxidation potential is deduced as 1.51 V_{RHE} for [SF–Fe–Co]. Considering a band gap of 2.25 eV (obtained from the zero-time delay of TA measurements, Figure 1a), the HOMO level for [SF–Fe] complex was found to be 2.42 V_{RHE}. (b) Proposed energy band diagram for [F_{OH}–SF–Fe–Co].

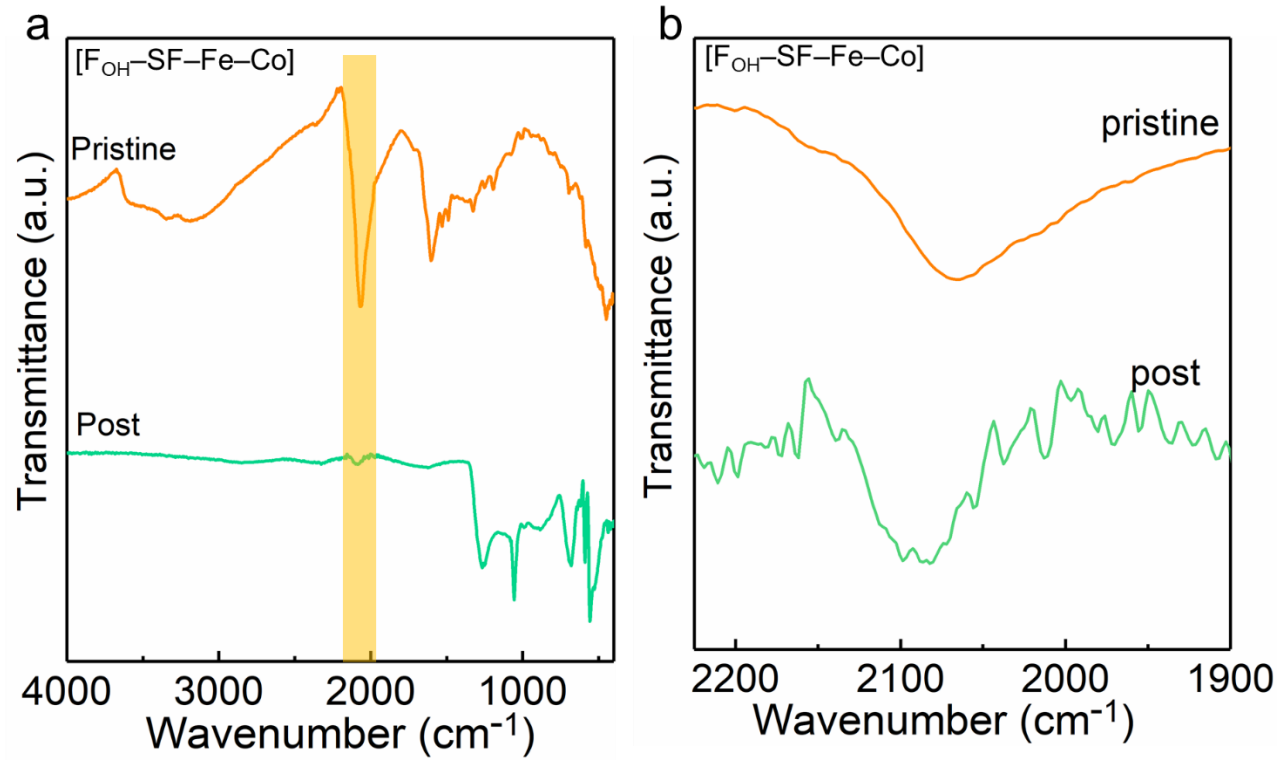

Figure S6. The Infrared spectra of both post-catalytic and pristine [F_{OH}–SF–Fe–Co] samples. The yellow line represents the cyanide peak region in (b). Notably, the post-catalytic sample exhibits additional broad peaks in the 1000–1200 cm^{-1} region. These peaks can be attributed to the incorporation of phosphate anions into the PB structure as counter ions, which serve to maintain charge balance in partially oxidized [F_{OH}–SF–Fe–Co] structure. The prominence of these peaks overshadows the others, causing the bands associated with water, cyanide, and organic groups to appear less dominant.

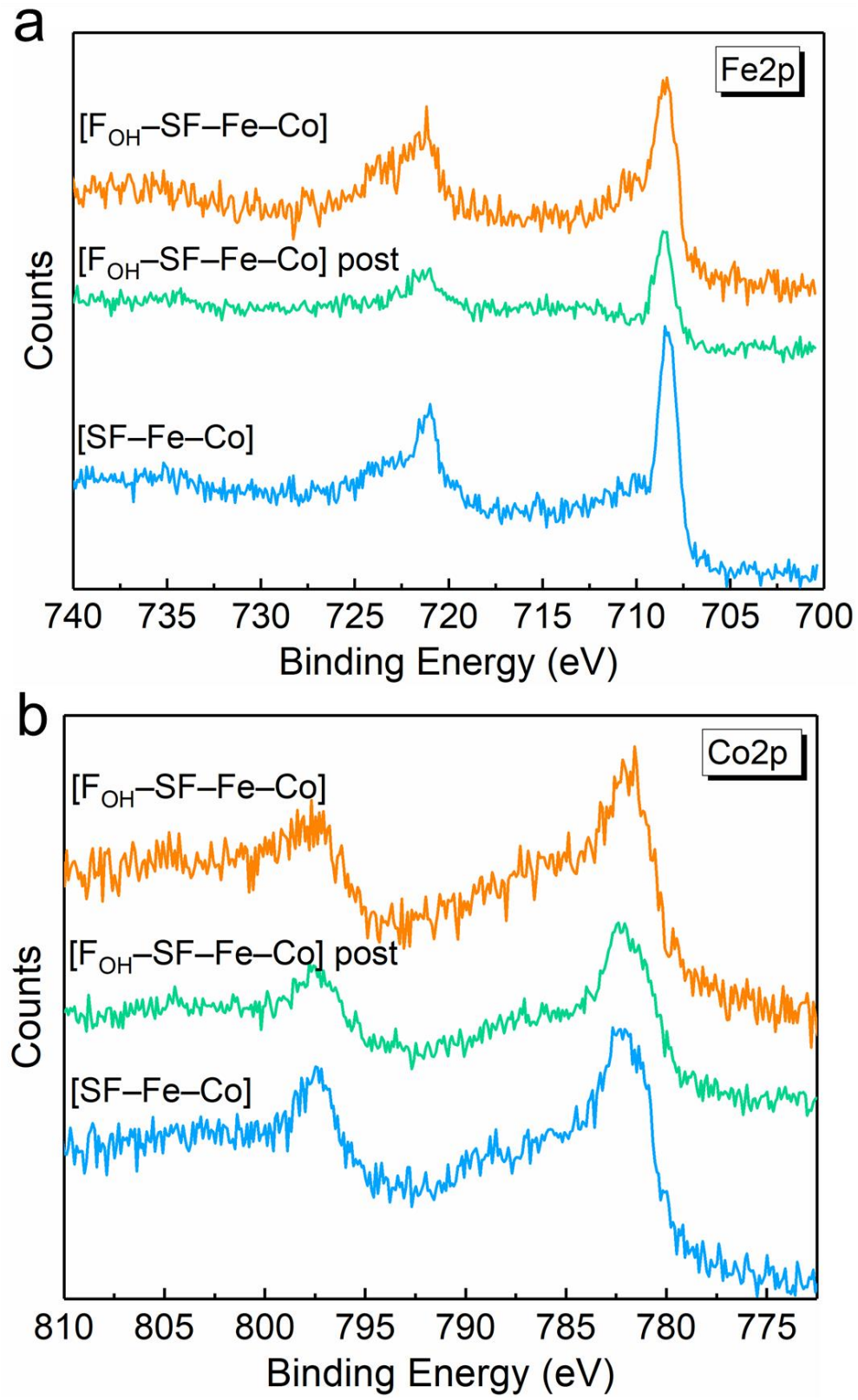

Figure S7. XPS analysis of [SF–Fe–Co] and pristine & post-catalytic [F_{OH}–SF–Fe–Co] samples: (a) Fe2p and (b) Co2p spectra.

Despite the inherent challenges in distinguishing oxidation states in high-resolution Co 2p spectra, encompassing both Co 2p1/2 and Co 2p3/2 regions, the Co 2+ state manifests at 797.0 eV and 781.4 eV for Co 2p1/2 and Co 2p3/2 signals, respectively.[1-9] Conversely, the Co 3+ state is evident at 799.4 eV and 782.6 eV for Co 2p1/2 and Co 2p3/2 signals, respectively. It should be also noted that the satellite peaks of Co 2p3/2 region is more obvious for Co 2+ and Co 3+ states at 784.8 and 788.1 eV, respectively. Although the disparity in oxidation states for Co 2p signals between F_{OH}-coordinated and non-coordinated catalytic sites is not pronounced, a subtle increase in the concentration of Co 3+ states is discernible in the post-catalytic [FOH–SF–Fe–Co] sample. In contrast, the Fe 2p signals in all samples exhibit more distinct peaks, facilitating a clearer distinction of oxidation states. In accordance with existing literature, the Fe 2+ state is identified at 721.2 eV and 708.2 eV for Fe 2p1/2 and Fe 2p3/2 regions, while the Fe 3+ state is observed at 723.4 eV and 709.9 eV for Fe 2p1/2 and Fe 2p3/2 regions, respectively.[10] Notably, there is no conspicuous difference in the oxidation states for Fe 2p signals between F_{OH}-coordinated and non-coordinated assemblies. However, a noteworthy reduction in the concentration of Fe 3+ sites is observed after photocatalytic reactions.

References

1. B. M. Pires, F. S. Hegner, J. A. Bonacin and J. R. Galán-Mascarós, ACS Appl. Energy Mater., 2020, **3**, 8448–8456.
2. T. G. Ulusoy Ghobadi, A. Ghobadi, M. Buyuktemiz, E. A. Yildiz, D. Berna Yildiz, H. G. Yaglioglu, Y. Dede, E. Ozbay and F. Karadas, Angew. Chemie, 2020, **132**, 4111–4119.
3. T. G. Ulusoy Ghobadi, E. Akhuseyin Yildiz, M. Buyuktemiz, S. Sadigh Akbari, D. Topkaya, Ü. İsci, Y. Dede, H. G. Yaglioglu and F. Karadas, Angew. Chemie - Int. Ed., 2018, **57**, 17173–17177.
4. T. G. U. Ghobadi, A. Ghobadi, M. Demirtas, R. Phul, E. A. Yildiz, H. G. Yaglioglu, E. Durgun, E. Ozbay and F. Karadas, Cell Reports Phys. Sci., 2021, **2**, 100319.
5. T. G. U. Ghobadi, A. Ghobadi, M. Demirtas, M. Buyuktemiz, K. N. Ozvural, E. A. Yildiz, E. Erdem, H. G. Yaglioglu, E. Durgun, Y. Dede, E. Ozbay and F. Karadas, Chem. - A Eur. J., 2021, **27**, 8966–8976.
6. T. Ivanova, A. Naumkin, A. Sidorov, I. Eremenko and M. Kiskin, J. Electron Spectros. Relat. Phenomena, 2007, **156–158**, 200–203.
7. C. Zhao, B. Liu, X. Li, K. Zhu, R. Hu, Z. Ao and J. Wang, Chem. Commun., 2019, **55**, 7151–7154.
8. S. S. Akbari and F. Karadas, ChemSusChem, 2021, **14**, 679–685.
9. S. S. Akbari, U. Unal and F. Karadas, ACS Appl. Energy Mater., 2021, **4**, 11, 12383–12390.
10. S. J. Gerber and E. Erasmus, Mater. Chem. Phys., 2018, **203**, 73–81.

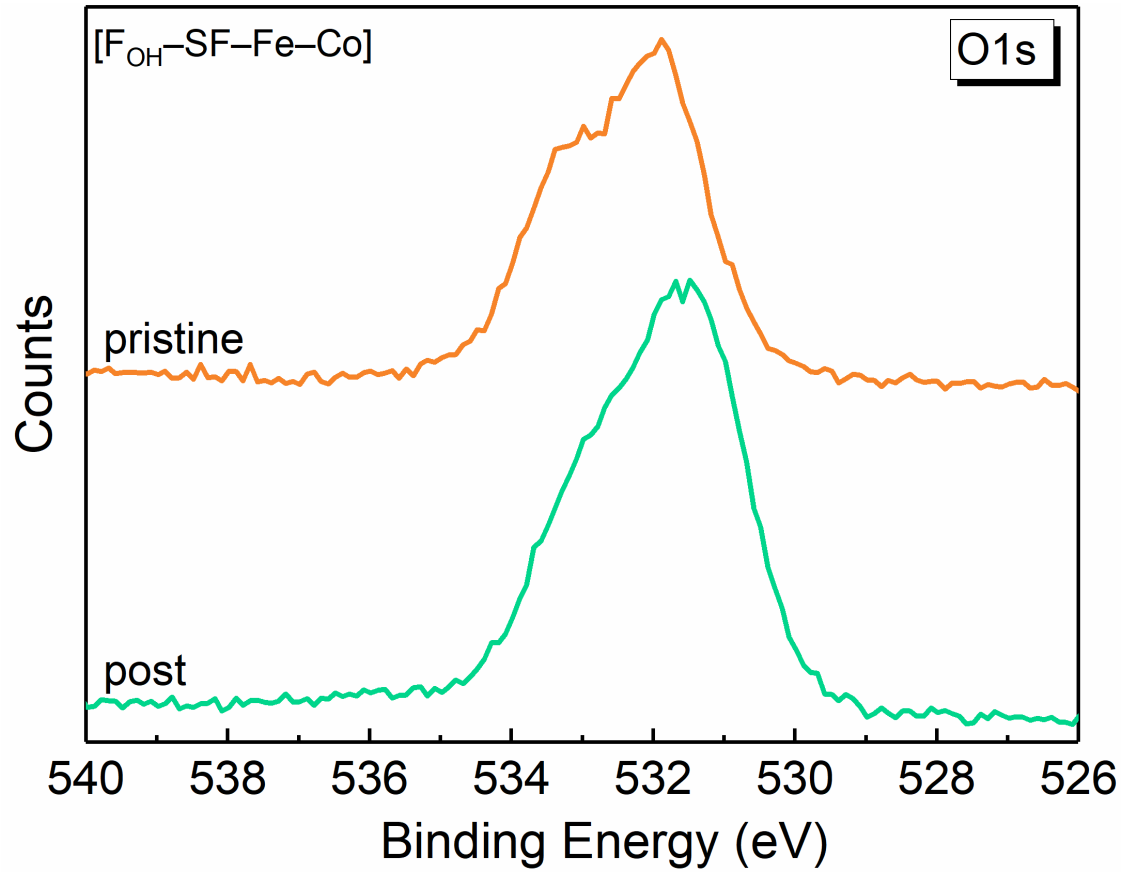

Figure S8. XPS analysis of O1s signals for post and pristine [F_{OH}–SF–Fe–Co] samples. The shift in the post O1s signal towards lower binding energies can be attributed to the incorporation of phosphate anions, whereas the Co sites do not exhibit any change in oxidation states in the post Co2p signal.